Potential energy surface for unimolecular dissociations and rearrangements of the ground state of systems (C 2 H 3 FO)

ARTICLE *in* PHYSICAL CHEMISTRY CHEMICAL PHYSICS · SEPTEMBER 1999

Impact Factor: 4.49

3 AUTHORS, INCLUDING:

Thanh Lam Nguyen

University of Texas at Austin

72 PUBLICATIONS **1,355** CITATIONS

SEE PROFILE

Minh Tho Nguyen

University of Leuven

747 PUBLICATIONS **10,295** CITATIONS

SEE PROFILE

PCCP

Potential energy surface for unimolecular dissociations and rearrangements of the ground state of $[C_2H_3FO]$ systems

Lam Thanh Nguyen,† Raman Sumathi and Minh Tho Nguyen*

Department of Chemistry, University of Leuven, Celestijnenlaan 200F, B-3001 Leuven, Belgium. E-mail: minh.nguyen@chem.kuleuven.ac.be

Received 11th September 1998, Accepted 13th November 1998

The potential energy surface (PES) of $[C_2H_3FO]$ systems in its electronic ground state has been investigated using density functional theory method, at the B3LYP/6-311++G(d,p) level. Ten stable intermediates, including acetyl fluoride (**1**), fluoroacetaldehyde (**9**), 1-fluorovinyl alcohol (**4**), 2-fluorovinyl alcohol, carbenes and fluorooxiranes, have been located. Most stationary points on the PES corresponding to the molecular elimination and rearrangement channels from these intermediates have been identified. Ketene (**8**) is found to be the predominant product in the unimolecular dissociations of **1**, **4**, **9** and fluorooxirane (**6**). The most probable channels for ketene formation from acetyl fluoride are **1** → **8** and **1** → **4** → **8**. In the reactions of both $CH_3CO^{\cdot}$ and $F^{\cdot}$ radicals, both these processes are energetically feasible for the thermal reactants and hence should lead to a spontaneous emission of vibrationally hot HF. The present PES characterises the $CH_3CO^{\cdot} + F^{\cdot}$ reaction to be a capture-limited association–elimination reaction with a very high and pressure-independent rate coefficient. In addition to its direct decomposition to ketene, **9** can give rise to stable rearrangement products, *viz*., 2-fluorovinyl alcohol (**12**) and **6**. Fluorooxirane (**6**) decomposes to ketene through its isomerisation to **9** as intermediate and the present study provides an explanation for the non-observation of this intermediate.

1 Introduction

The study of unimolecular dissociation and its precursor intramolecular vibrational energy redistribution (IVR) has long been a topic of both experimental and theoretical molecular dynamics. Of particular recent interest, in addition to the qualitative understanding of a chemical reaction and the ability to predict the branching between the energetically allowed product channels, is the possibility of mode-specific chemistry, where the excitation of a particular vibrational mode leads to an enhanced rate of reaction.[1] Formaldehyde,[2] acetaldehyde,[3,4] acetyl chloride[5,6] and fluoroformaldehyde[7–9] are the few prototypical carbonyl compounds in which photochemical and thermal dissociations, involving the ground and excited state surfaces, have been studied extensively by both experiment and theory.

Recent experimental studies would seem to indicate that HFCO would be a good candidate for vibrationally enhanced, mode-specific unimolecular dissociation. Moore *et al.*[8] have carried out a series of stimulated emission pumping (SEP) experiments, studying the dissociation of vibrationally excited HFCO on the ground S_0 surface. Unimolecular dissociation rates of HFCO were measured[8c] for well characterised initial rovibrational states which showed a clear evidence of mode specificity at higher energies. They have also characterised the energy distributions of the CO dissociation products.[8d] In spite of the rapid development in the experimental techniques to probe the reaction dynamics, the understanding of the dissociation dynamics of polyatomic molecules is still in its infancy.

Substitution of a methyl group instead of a hydrogen of HFCO leads to the next member, CH_3COF, in the homologous series of carbonyl compounds; this substitution, however, is expected to introduce experimental difficulties owing to its complex dissociation and rearrangement channels as well as *via* strong vibrational mixing. We are not aware of any experimental work on the dissociation dynamics of acetyl fluoride. Recently, one of its isomers, fluorooxirane, has been synthesised[10] and its structure has been derived from high resolution infrared spectroscopic data. It is shown from the spectroscopic and kinetic data that CH_2OCHF decomposes[10,11] during and after multiphoton excitation to give ketene and hydrogen fluoride. This elimination could be a direct or a complex elimination *via* the initial rearrangement to acetyl fluoride or fluoroacetaldehyde intermediates. *Ab initio* calculations[11] using the CCSD(T)/6-311G(d,p)//MP2/6-311(d,p) method were performed on this chiral oxirane molecule to explain the observed laser chemical reaction dynamics, *viz*., the absolute laser chemical reaction rate coefficient and the branching ratios for various reaction channels. Inconsistencies, however, still exist between the experimental observations and the theoretical predictions with respect to the product branching ratios. As well as the ketene product, several other products are equally possible but they have not been taken into consideration in ref. 11. Earlier theoretical investigations[12–18] on the $[C_2H_3FO]$ systems have mainly been confined to the conformational analysis and prediction of vibrational wavenumbers and thermochemical parameters.

As a first necessary step towards an understanding of the reaction dynamics of $[C_2H_3FO]$ isomers, we wish to establish its potential energy surface (PES) as completely as possible. In this regard, we consider here the possible decomposition, isomerisation and dissociation channels on the lowest lying singlet state energy surface of acetyl fluoride and its rearranged isomers, namely fluoroacetaldehyde, 1-fluorovinyl alcohol, 2-fluorovinyl alcohol, carbonyl ylides and fluorooxirane. Moreover, since the system involves four heavy

† Permanent address: Faculty of Chemical Engineering, Ho Chi Min City University of Technology, Vietnam.

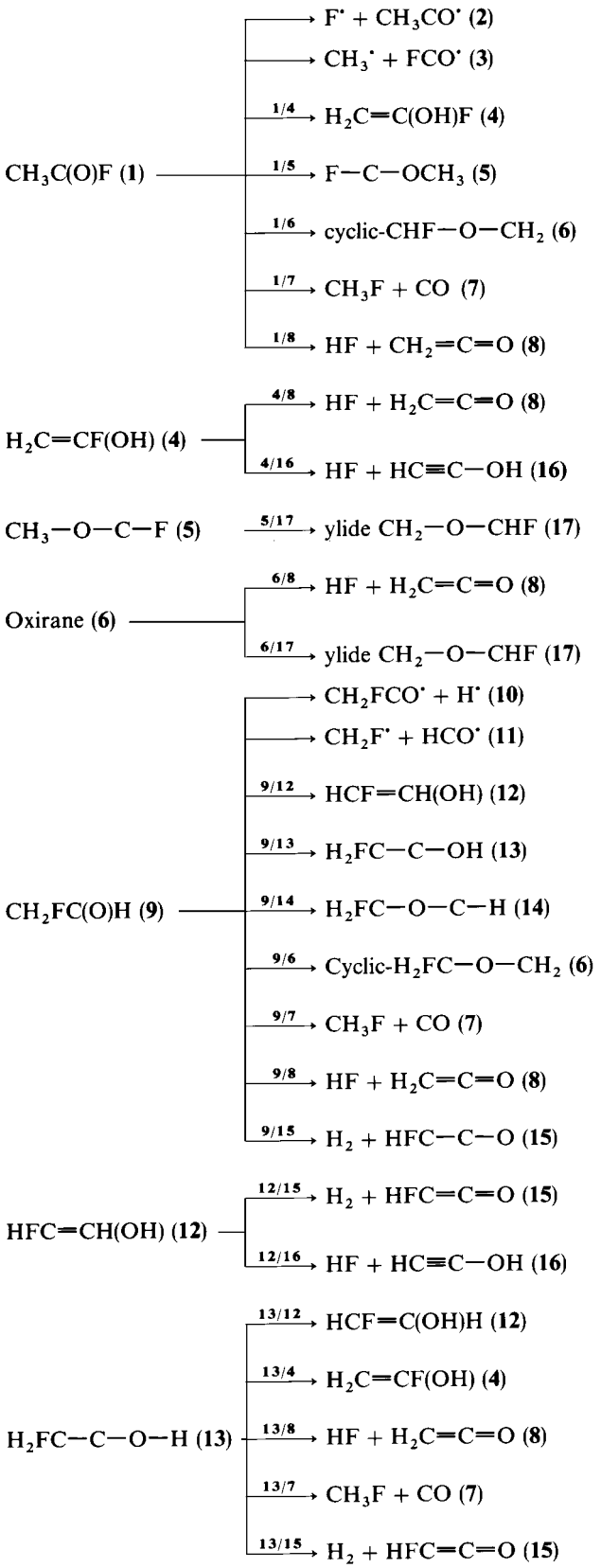

Scheme 1

atoms and the fact that our interests are in characterising all stationary points on the surface at a uniform and reliable level of treatment, we adopt here the computationally less demanding density functional theory (DFT) approach. The different reactions considered in the present investigation are shown in Scheme 1. The purpose of this work is to determine these unimolecular rearrangement and dissociation pathways and their barrier heights. To achieve this, it is necessary to determine the geometries of the reactants, and the saddle points for the various reactions and their products. A comparison of the results has been made with the earlier *ab initio* results reported for the decompositions of HFCO,[9,19] CH_3CHO,[4] CH_3COCl[6] and CH_3COCN.[20] In the last section, we qualitatively explain the kinetics of $CH_3CO + F$ reaction, one of the entrance channels on the $[C_2H_3OF]$ PES. Furthermore, the kinetics of the chlorine analog of this reaction, $CH_3CO + Cl$, has derived considerable interest in recent years. The real-time kinetic measurements on $CH_3CO + Cl$ reaction have been made recently by Maricq *et al.*[21] over a pressure range of 10–200 Torr and a temperature range of 215–353 K. They identified ketene as a product but could not distinguish between addition–elimination and direct abstraction mechanisms of formation. Hence, it is worth comparing the kinetics of $CH_3CO + F$ and $CH_3CO + Cl$ reactions to derive some additional insights. In relation to recent experimental studies on fluorooxirane,[10,11] particular attention is also paid to its decomposition processes.

2 Computational details

All calculations were performed using the GAUSSIAN 94 program.[22a] Geometries of reactants, adducts and transition state structures were optimised using density functional theory with the popular hybrid B3LYP functional in conjunction with analytical gradient methods. The exchange functional[22b] in the hybrid B3LYP method consists of three terms, including the Hartree–Fock exchange functional. The correlation functional is that of Lee, Yang and Parr.[22c] The open shell calculations were performed using the unrestricted formalism (UHF, UB3LYP). The PES was initially mapped out with B3LYP/6-31G** calculations. The identity of each first order stationary point is determined when necessary by intrinsic reaction coordinate (IRC) calculations. Geometries were then reoptimised with a larger (6-311++G(d,p)) basis set. The zero-point energies were derived from harmonic vibrational wavenumbers at the (U)B3LYP/6-31G** level. Throughout this paper, bond lengths are given in angströms, bond angles in degrees, and zero point and relative energies in kcal mol^{-1}, unless otherwise stated.

3 Results

The results of the present investigation will be discussed under the following sections: (1) equilibrium structure of the intermediates, (2) PES of acetyl fluoride (**1**) and fluoroacetaldehyde (**9**), (3) PES of 1-fluoro (**4**) and 2-fluorovinylalcohol (**12**), (4) PES of carbenes, (5) PES of fluorooxirane and (6) mechanism of ketene formation and comparison of both $CH_3CO + F$ and $CH_3CO + Cl$ reactions. The B3LYP/6-311++G(d,p) optimised geometries of the stable intermediates, *viz.*, **1**, **9**, **4**, **12**, carbenes (**5**, **13**, **14**), fluorooxirane (**6**) and ylides (**17**) are shown in Fig. 1. The transition structures (TSX/Y) are numbered with both the reactant (***X***) and product (***Y***) numbers. The optimized geometries of the saddle points on the PES of **1** are shown in Fig. 2 whereas those of **9** are shown in Fig. 3. Fig. 4 displays the saddle point geometries on the PESs of **4** and **12**. The optimized geometries of the saddle points on the PES of carbenes and fluorooxiranes are displayed, respectively, in Figs. 5 and 6. The schematic representation of the potential energy surface for the $[C_2H_3FO]$ system is shown in Figs. 7 and 8. The relative energies displayed correspond to B3LYP/6-311++G(d,p) values corrected for zero-point energies (ZPE) using B3LYP/6-31G(d,p) frequencies and are relative to the ground state of **1** and they represent our best estimates for relative energies and will thus be employed in the following

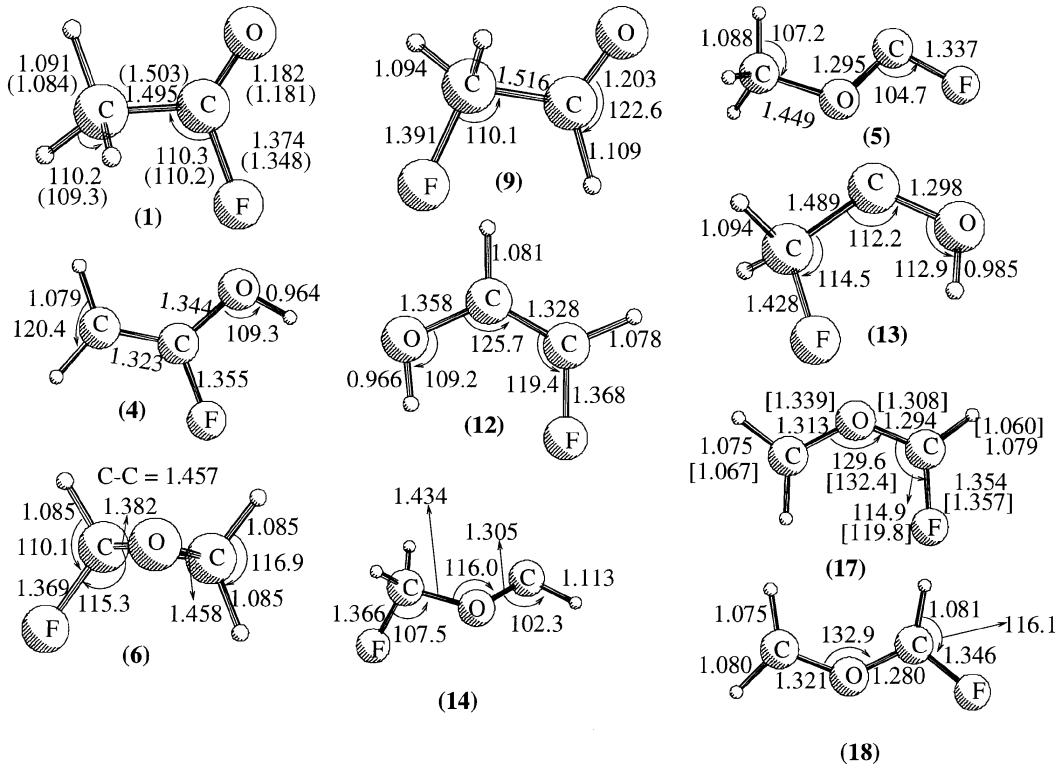

Fig. 1 Selected B3LYP/6-311++G(d,p) optimised geometries of the intermediates on the $[C_2H_3FO]$ PES. The numbers within parentheses correspond to the experimental values for **1** from ref. 23 and square brackets the TCSCF/4-31G values from ref. 33 for **17**.

discussion. The harmonic vibrational frequencies of the stationary points along with their rotational constants are in Tables 1–3. In addition to the reactions depicted in Scheme 1, we have also considered the numerous internal rotation barriers in all the likely intermediates on the $[C_2H_3OF]$ PES; however, to simplify the presentation, the corresponding TSs are not given and only the barriers will be mentioned in the text.

4 Discussion

4.1 Equilibrium structure of the intermediates

The microwave spectrum of acetyl fluoride (**1**) was first reported by Pierce.[23] There is a general consensus, based on microwave spectroscopic,[24] gas electron diffraction,[25] infrared spectroscopic[26] and *ab initio* investigations that, in CH_3COX (X = H, OH, CH_3, NH_2 or halogens) systems, one of the methyl C—H bonds is in an eclipsed arrangement with the C=O group, yielding a *syn*-planar H—C—C=O configuration. In the present study, we have observed the same preference in conformation. The height of the threefold barrier to internal rotation was calculated to be close to 1.07 kcal mol^{-1}. The *ab initio* and experimental[23] bond lengths and angles of **1** are shown in Fig. 1. The C—O and C—C bond lengths are in very good agreement with the experiment. A major deviation of 0.026 Å has been observed for the C—F bond length. This deviation, in combination with the shorter C—O bond length (*e.g.*, the C—O bond length in **1** is 0.03 Å shorter than that in acetaldehyde or acetyl chloride), suggests

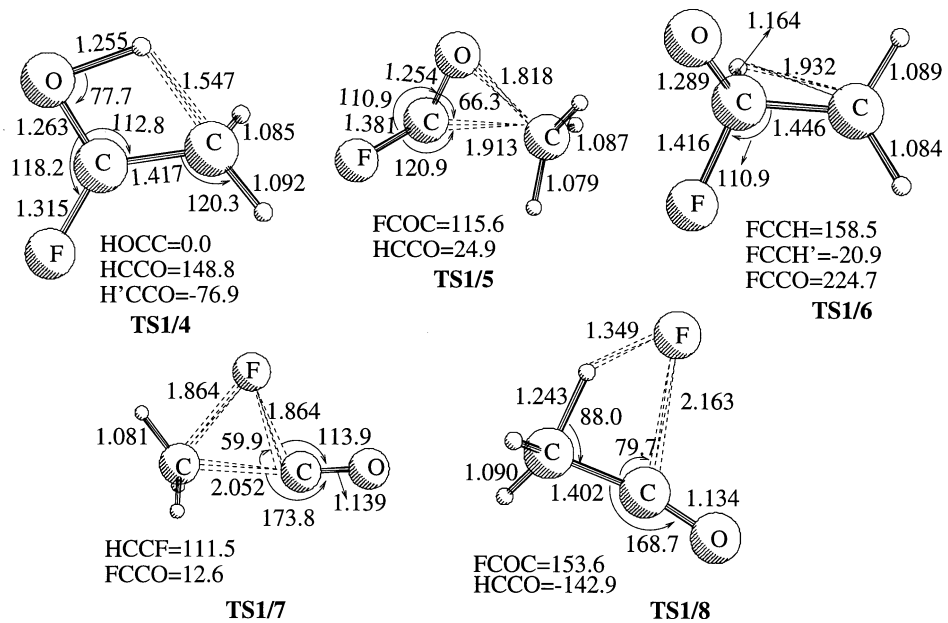

Fig. 2 Selected B3LYP/6-311++G(d,p) optimised geometries of the transition structures **1**/**4**, **1**/**6**, **1**/**7** and **1**/**8** relevant to the CH_3COF (**1**) PES.

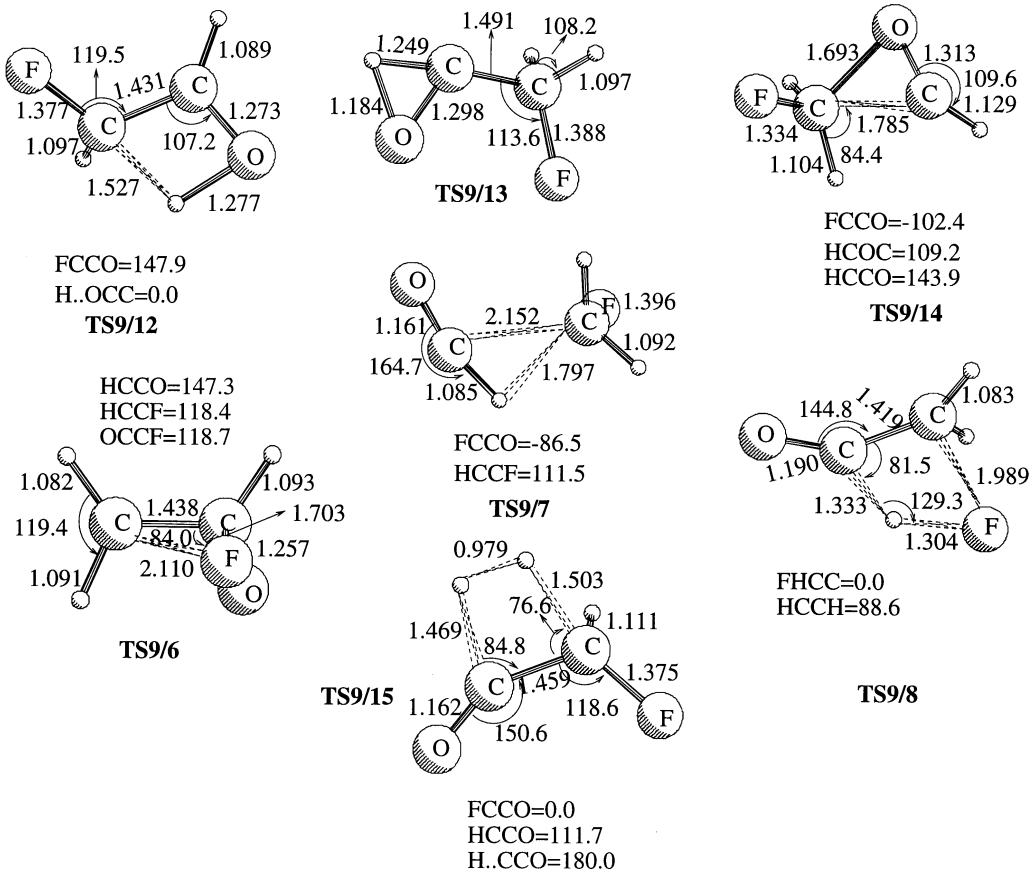

Fig. 3 B3LYP/6-311++G(d,p) optimised geometries of the transition structures **9**/**12**, **9**/**13**, **9**/**14**, **9**/**15**, **9**/**6**, **9**/**7** and **9**/**8** relevant to the CH_2FCHO (**9**) PES.

the probable importance of the ionic form $CH_3CO^+F^-$. However, multiconfigurational calculations are needed to establish its extent of contribution. It is worth mentioning that the associated experimental uncertainties in the C—F bond length are quite large (±0.015 Å). The calculated molecular rotational constants for **1** are $A = 10.918$, $B = 9.652$ and $C = 5.290$ GHz and are in good agreement with the experimental microwave data of 11.039, 9.685 and 5.322 GHz, respectively. The calculated C—C bond length of 1.495 Å indicates a partial double bond character as it is shorter than the C—C single bond length in ethane (1.543 Å) and longer than the C=C length in ethylene (1.339 Å). All fifteen modes of **1** are infrared active and they transform as 10a′ and 5a″ modes under the symmetry operations of the C_s point group. The characteristic C—C, C—F and C=O stretching absorptions are found to resonate, respectively, at 1014, 1231 and 1932 cm^{-1}.

Fluoroacetaldehyde (**9**) is apparently unstable at ambient temperature in pure form and, therefore, no experimental data are available. The conformational stability, structural parameters and barriers to internal rotation of **9** were studied earlier at the RHF/6-31G* and MP2/6-31G* levels by Phan and Durig.[27] In agreement with this previous investigation, we found that the *cis*-conformer, wherein the fluorine atom and the aldehydic hydrogen eclipsed one another, to be more stable than the *trans*-conformer. The energy difference between these two conformers is around 1.4 kcal mol^{-1}. The F—CH_2 bond length in **9** (1.391 Å) is longer than the C(O)—F distance in **1** (1.374 Å). The barrier to internal rotation around the C—C bond has been calculated to be 4.95 kcal mol^{-1}. The characteristic C—C, C—F and C=O stretching vibrations are calculated to absorb, respectively, at 1035.7, 1108.9 and 1843.3 cm^{-1} (Table 1).

The optimised geometry of the most stable conformer of 2-fluorovinyl alcohol (**12**) is shown in Fig. 1. We have investigated four conformers of this molecule, *viz*., *cis-syn*, *cis-anti*, *trans-syn* and *trans-anti*. The most stable structure is the *cis-syn* isomer and the internal hydrogen bond in this conformer is responsible for its stabilisation. The *cis* isomer has greater thermodynamic stability over the *trans* isomer due to the presence of the electronegative vicinal substituents (so-called "*cis* effect"). The *trans* isomer has been characterised as a transition state. The energy difference between the *cis-syn* and *cis-anti* isomers is 3.4 kcal mol^{-1}. These results are in good agreement with the earlier conformational study on **12** at the Hartree–Fock level by Dixon *et al.*[28]

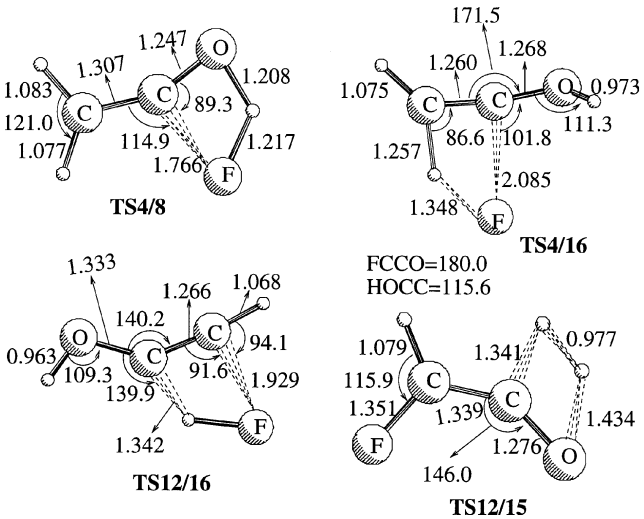

Fig. 4 B3LYP/6-311++G(d,p) optimised geometries of the transition structures **4**/**8**, **4**/**16**, **12**/**16** and **12**/**15** relevant to the H_2C=CF(OH) (**4**) and HFC=C(OH)H (**12**) PESs.

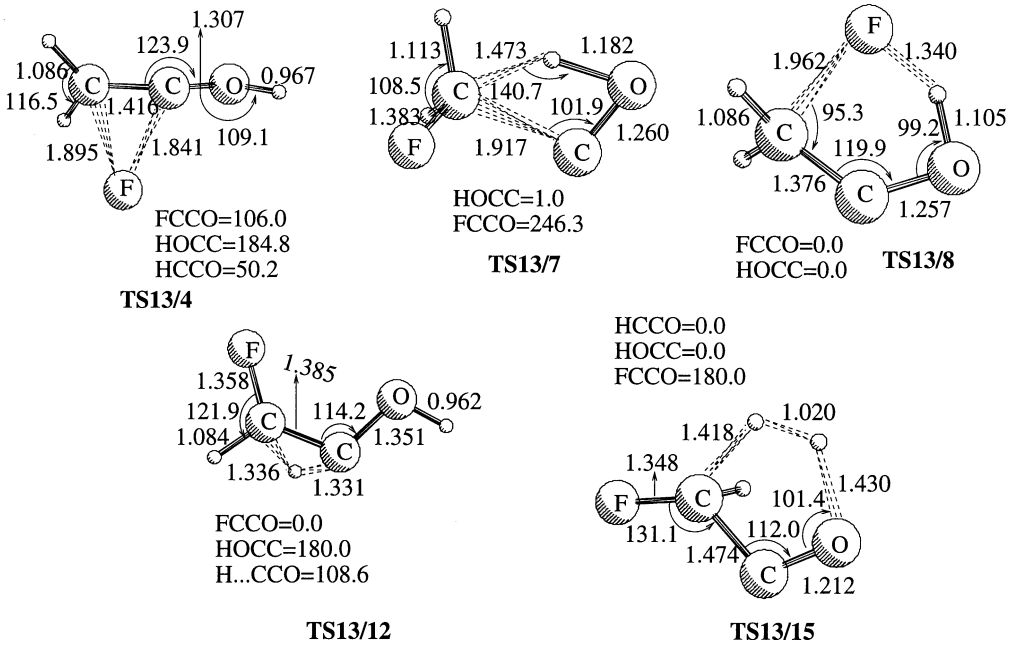

Fig. 5 B3LYP/6-311++G(d,p) optimised geometries of the transition structures **13/4**, **13/7**, **13/8**, **13/12** and **13/15** relevant to the H_2FCCOH carbene PES.

The optimised geometry of 1-fluorovinyl alcohol (**4**) is shown in Fig. 1. The *cis* orientation of hydrogen is slightly preferred over the *trans* orientation again due to internal hydrogen bonding and this conformation is more apt for the *syn*-elimination of hydrogen fluoride. The hydrogen bonded distance, H···F, in **4** is 2.186 Å while in **12** the corresponding distance is slightly larger, 2.341 Å, and thereby signifies a stronger interaction in the former compared with the latter. The transition state for the *syn-anti* isomerisation is found to lie 3.6 kcal mol^{-1} above the most stable *cis* isomer.

Calculations of the equilibrium geometry of fluorooxirane (**6**) have been reported earlier at MP2/TZ2P level of calculation and compared with the experimental values.[11] The B3LYP values are very close to their optimized geometry at MP2/6-311G(d,p) level (see column 3 of Table 1 in ref. 11). Fluorooxirane is thermodynamically less stable by 43.6 kcal mol^{-1} compared with **1**. However, its stability as a discrete molecule depends upon the kinetic barriers involved in its dissociation. Ha *et al.*[11] have found appreciable barriers for its dissociation to **1** or **9** which in turn explain the experimental characterisation of this species. The importance of this intermediate in the kinetics of the unimolecular reaction dynamics of **1** or **9** depends on the barrier height for its formation and will be examined in a subsequent section.

In contrast to the parent methylene ($^{\cdot\cdot}CH_2$), carbenes which contain an oxygen atom directly attached to the electron deficient carbon exhibit singlet ground electronic states. This is owing to the resonance stabilising effect of the lone pairs of electrons on the oxygen. The carbenes derived from formaldehyde[29] and fluoroformaldehyde,[30] *viz.*, hydroxymethylene and fluorohydroxymethylene, have been observed experimentally. Methoxychlorocarbene, which could be derived from acetyl chloride, has been identified experimentally by a matrix isolation technique[31] and its vibrational frequencies from the IR spectra have been reported. Previous calculations on hydroxyfluorocarbene,[9] methoxycarbene,[32] methoxychlorocarbene,[6] chlorohydroxymethylcarbene,[6] methoxycyanocarbene[20] and methoxyisocyanocarbene[20]

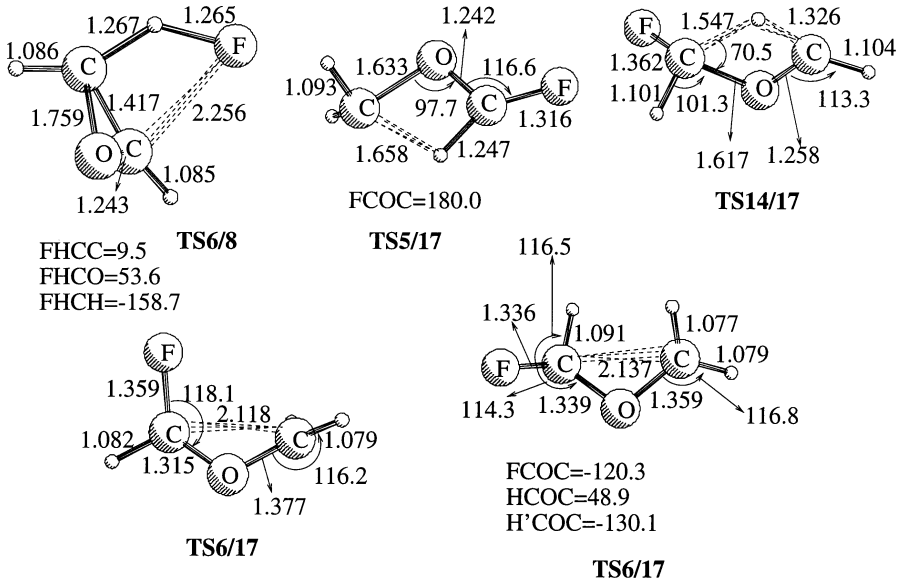

Fig. 6 B3LYP/6-311++G(d,p) optimised geometries of the transition structures **6/8**, **5/17**, **14/17** and **6/17** relevant to the fluorooxirane (**6**) PES.

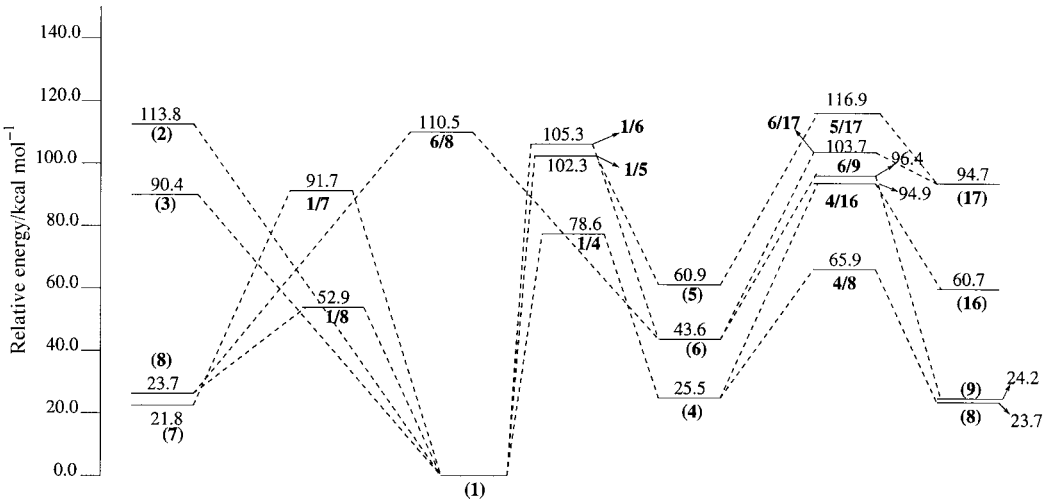

Fig. 7 The overall profile of the PES related to the $[C_2H_3FO]$ system, including the reactions from the intermediates **1**, **6**, **4** and **5** calculated at the B3LYP/6-311++G(d,p)+ZPE level of theory.

suggest the existence of both *cis* and *trans* isomers. We have analysed both the *cis* and *trans* isomers of methoxy-fluorocarbene (**5**), $CH_2F{-}C{-}O{-}H$ (**13**) and $CH_2F{-}O{-}C{-}H$ (**14**). The *cis-trans* isomerisation transition states are not given here for the sake of conciseness. The transition state structures for internal rotations between the *cis* and *trans* forms of singlet methylene isomers have their torsional angles very close to 90°. The barriers for internal rotation in **5**, **13** and **14** are calculated to be 19.7, 26.8 and 26.7 kcal mol^{-1}, respectively. Singlet *trans*-CH_3OCF (**5**) and **14** have a OCX (X=F,H) bond angle of 104.7° (X=F) and 102.2° (X=H), which are typical of a singlet carbene. The

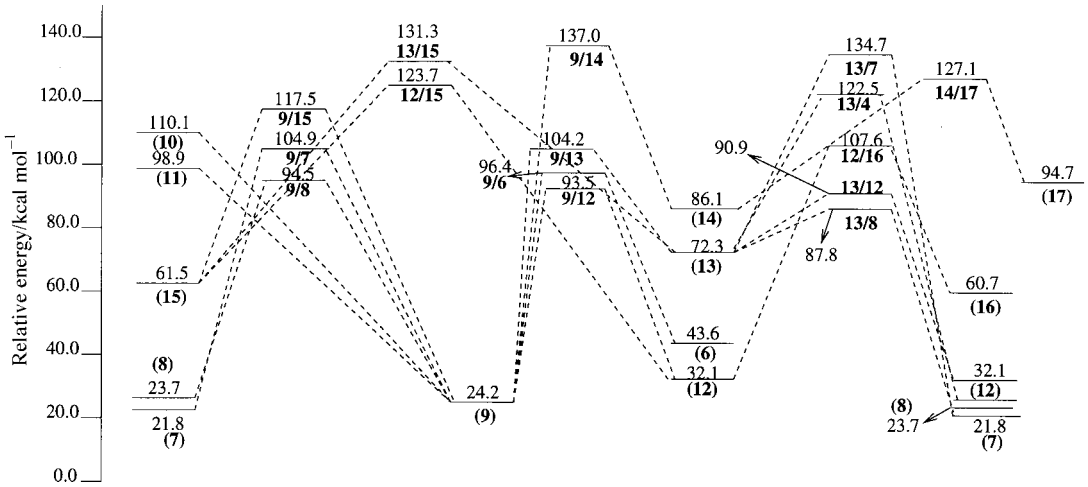

Fig. 8 The overall profile of the PES related to the $[C_2H_3FO]$ system, including the reactions from the intermediates **9**, **12**, **13** and **14** calculated at the B3LYP/6-311++G(d,p)+ZPE level of theory.

Table 1 Unscaled B3LYP/6-31G(d,p) harmonic vibrational frequencies of the various intermediates on the PES of (C_2, H_3, O, F) system; zero-point energies (ZPE) are given in kcal mol^{-1}

Species	Frequencies/cm^{-1}	ZPE
1	125.4, 410.2, 561.5, 597.1, 851.9, 1013.6, 1070.7, 1230.6, 1411.1, 1480.3, 1489.4, 1932.4 3072.3, 3150.4, 3166.9	30.8
4	111.9, 437.1, 523.9, 627.8, 718.7, 773.8, 927.4, 970.4, 1199.6, 1368.4, 1428.8, 1807.6 3216.9, 3317.2, 3829.6	30.4
5	155.9, 242.9, 356.1, 609.7, 1047.0, 1161.4, 1172.5, 1186.4, 1340.6, 1479.5, 1502.9, 1515.7, 3070.1 3162.3, 3169.7	30.3
6	428.9, 507.3, 799.2, 889.5, 982.3, 1101.2, 1140.3, 1163.7, 1184.4, 1317.9, 1435.5, 1539.2, 3110.0 3154.4, 3207.5	31.3
9	83.6, 314.5, 530.8, 715.8, 1035.7, 1108.9, 1112.3, 1244.6, 1355.6, 1411.6, 1484.6, 1843.3, 2922.1 3040.5, 3089.1	30.4
12	229.4, 438.7, 522.7, 727.6, 760.7, 878.7, 1033.5, 1125.1, 1232.3, 1368.7, 1417.4, 1766.0, 3237.9, 3270.2 3783.8	31.1
13	263.9, 325.2, 712.2, 744.6, 877.3, 990.0, 1002.9, 1235.4, 1346.9, 1374.1, 1406.9, 1460.9, 3055.6 3105.7, 3411.8	30.5
14	98.5, 447.5, 504.6, 738.4, 962.3, 1144.9, 1169.6, 1270.9, 1328.5, 1433.6, 1459.9, 1536.1, 2836.4 3067.2, 3149.1	30.2
17	248.3, 422.5, 484.8, 583.4, 614.8, 692.5, 1112.6, 1153.0, 1219.4, 1374.2, 1476.8, 1512.9, 3204.5 3226.9, 3357.1	29.6

C—O distance of 1.295 Å reflects the partial double bond character. The *cis-trans* isomerisation is nearly thermoneutral in CH_2FCOH carbene and in both the isomers the C—F bond is eclipsed with the C—O bond. The partial double bond character is reflected by the C—O distance (1.299 Å).

The characterisation of the structure and energetics of the ylides is generally difficult because they might exist in both zwitterionic and biradical states. The optimized geometry of the isomers of the ylides is shown in Fig. 1 along with the TCSCF/4-31G optimised geometries from ref. 33. The stable isomer takes the *cis* form wherein the fluorine can interact with the hydrogen attached to the other carbon. The CHF—O distance is shorter (1.294 Å) than the CH_2—O distance (1.313 Å). A similar observation has already been made by Tachibana *et al.*[33] in their study on the dynamic stability of carbonyl ylides at the MCSCF level of treatment using the 4-31G basis set. It is interesting to note that the density functional approach is able to describe this multiconfigurational system to a good extent.

4.2 PES of 1 and 9

Both **1** and **9** can undergo unimolecular rearrangements, molecular eliminations and radical dissociation channels. As shown in Scheme 1, the various possible unimolecular rearrangements include (a) the 1,3-migration of hydrogen, (b) the 1,2-migration of CH_2X (X = H,F), (c) the 1,2-migration of X (X = H,F) and (d) the simultaneous migration and ring closure to oxiranes. Each of these rearrangements will be discussed in detail below.

4.2.1 Unimolecular rearrangements: keto-enol tautomerism.

$$CH_3C(O)F\ (\mathbf{1}) \xrightarrow{1/4} CH_2C(OH)F\ (\mathbf{4})$$

$$CH_2FC(O)H\ (\mathbf{9}) \xrightarrow{9/12} CHFC(OH)H\ (\mathbf{12})$$

This prototropic rearrangement formally involves the migration of a hydrogen α to a carbon-heteroatom double bond to the heteroatom and thereby leads to the formation of a C=C double bond. In other words, it involves 1,3-hydrogen migration from the methyl group to the carbonyl oxygen, giving rise to vinyl derivatives. Thermodynamically, this reaction is less endothermic compared with other unimolecular rearrangement processes from **1** (Fig. 7). The keto tautomers **1** and **9** are lower in energy than their enol counterparts (**4** and **12**) by roughly 25.5 and 7.9 kcal mol^{-1}, respectively, indicating that the tautomeric equilibrium lies heavily to the keto side. Transition structure searches for the hydrogen migration from carbon to oxygen located the TS **1**/**4** and **9**/**12**; as shown in Figs. 2 and 3, they are four-membered transition structures and all four atoms lie in approximately the same plane.

The migrating hydrogen in **1**/**4** is 1.255 and 1.547 Å, respectively, away from the migrating terminus and origin. The reaction coordinate has been identified as the asymmetric C···H—O stretch and the magnitude of the vibration which has been lost at the transition state equals 2030.1i cm^{-1} (Table 2). The transition structure is energetically disposed above the reactant minimum, **1** by 78.6 kcal mol^{-1} and it lies below both the C—C and C—F bond dissociation limits. However, it is roughly 25.7 kcal mol^{-1} above the transition structure **1**/**8** for the dissociation into ketene and hydrogen fluoride. Hence, the predominant channel for the disappearance of **1** seems to be the molecular dissociation to ketene and HF *via* **1**/**8**. However, if one studies the kinetics of the reaction between $CH_3CO^{\cdot} + F^{\cdot}$, one of the entrance channels to the CH_3COF minimum, using this PES, has as an initial step a fast barrierless recombination of the radicals to yield the energised CH_3COF (**1***) with an excess energy of 113.8 kcal mol^{-1}. The energised **1*** would then undergo a competitive isomerisation (to **4**) and elimination (of HF) reactions with a product branching ratio which is dependent on the ratio of their barrier heights as well as on the partition functions of the respective transition states. Both the transition states **1**/**4** and **1**/**8** are equally tight and the calculated preexponential factors for both the processes are 2.56×10^{12} and 5.76×10^{12} s^{-1}, respectively. Preexponential factors were calculated as

$$A_i = \frac{k_B T}{h} \frac{Q_i^{\dagger}}{Q_i}$$

where k_B is the Boltzmann constant, h is Planck's constant, T the temperature in Kelvin and $Q_i^{\dagger}$ and Q_i are the complete partition functions for the respective transition state and the reactant, respectively. The partition functions were obtained from the B3LYP level calculated harmonic vibrational frequencies and moments of inertia. These results indicate a competitive formation of $CH_2CO + HF$ and **4**, with a preference for the former. However, once formed, **4** will have more energy than the barrier for its dissociation (since **4**/**8** lies below **1**/**4**) and hence will spontaneously dissociate into ketene and HF.

Table 2 Unscaled B3LYP/6-31G(d,p) harmonic vibrational frequencies of the various saddle points on the acetyl fluoride (**1**) PES; zero-point energies (ZPE) are given in kcal mol^{-1}

Species	Frequencies/cm^{-1}	ZPE
1/**4**	2030.1i, 452.2, 492.7, 550.3, 717.9, 798.9, 995.1, 1070.3, 1153.8, 1385.0, 1499.7, 1594.5, 2004.8 3102.5, 3195.9	27.2
1/**5**	819.5i, 150.5, 287.8, 527.3, 646.4, 927.1, 985.9, 1057.2, 1302.0, 1439.4, 1460.4, 1495.7, 3082.3 3173.7, 3283.2	28.3
1/**6**	1352.6i, 348.5, 492.1, 587.1, 807.2, 889.8, 1040.2, 1078.0, 1138.5, 1278.6, 1298.4, 1490.2, 2296.1 3130.2, 3272.2	27.4
1/**7**	834.8i, 67.7, 174.0, 281.3, 459.7, 584.8, 981.4, 1018.7, 1297.4, 1465.9, 1507.9, 2057.0, 3117.7 3245.4, 3273.6	27.9
1/**8**	1566.3i, 300.9, 369.6, 452.6, 613.9, 696.4, 885.9, 1044.4, 1078.1, 1306.3, 1438.4, 1869.8, 2190.6 3124.0, 3206.2	26.5
4/**8**	1638.9i, 346.9, 445.9, 545.9, 617.6, 693.5, 738.5, 933.2, 995.9, 1186.5, 1427.6, 1927.7, 2088.9, 3207.3 3320.2	26.4
4/**16**	1693.3i, 243.4, 356.4, 412.4, 593.9, 624.5, 708.5, 809.2, 964.9, 1097.8, 1236.4, 1813.9, 2019.9, 3315.5 3724.9	25.6
5/**17**	1235.6i, 41.6, 394.8, 481.7, 635.3, 715.1, 1127.4, 1172.0, 1187.8, 1258.4, 1437.8, 1639.9, 2277.1 3036.8, 3129.2	26.5
6/**8**	1229.9i, 267.1, 395.8, 445.6, 731.3, 821.5, 974.4, 1049.4, 1121.4, 1189.2, 1355.6, 1564.6, 1813.6 3164.5, 3223.0	25.9
6/**17**	316.3i, 304.5, 389.2, 559.6, 660.9, 772.4, 1103.6, 1176.5, 1178.3, 1268.6, 1363.9, 1517.0, 3079.1 3181.5, 3334.3	28.4

The analogous isomerisation in fluoroacetaldehyde, *viz.*, **9** → **12**, is less endothermic and involves a relatively lower barrier height of 69.3 kcal mol^{-1}. The nature of **9**/**12** is very similar to that of **1**/**4** and the magnitude of the imaginary frequency equals 2066.6i cm^{-1} (Table 3). The importance of these intermediates (**4** and **12**) in the elimination of HDF from **1** will be discussed a little later.

4.2.2 Rearrangement to carbenes.

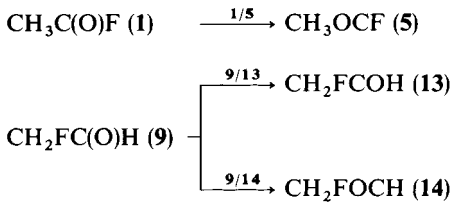

The carbene **5** could be derived from **1** *via* the 1,2-migration of the methyl group. As can be seen from Fig. 7, the energy barrier (102.3 kcal mol^{-1}) to produce this carbene from **1** is quite high. Moreover, one of the bond dissociation limits of **1**, namely $CH_3^{\bullet}$ + FCO$^{\bullet}$, lies energetically lower than this transition structure **1**/**5** (90.4 kcal mol^{-1}). Therefore, most of the $CH_3(O)F$ molecules with energy equal to or greater than 90.4 kcal mol^{-1} would prefer to dissociate over migration and this preference is additionally aided by the larger magnitude of the preexponential factor for the dissociation. However, it is interesting to note from Fig. 7 that the carbene **5**, once formed, has sufficient stability and long lifetime, owing to the high reverse barrier for the formation of **1**. The structure of the transition state **1**/**5** is shown in Fig. 2 for the sake of completeness. The other possible carbene, CH_3COF, which can arise from **1** *via* 1,2-migration of fluorine is highly unstable, indicating a very weak O—F bond, and we have not been successful in obtaining the equilibrium structure of this carbene. The corresponding carbene from formyl fluoride, HCOF, was also found to be unstable and its structure has been regarded as a complex of HCO with F.

The carbenes **13** and **14** can be derived from **9** by the respective 1,2-migration of H and CH_2F groups from the carbon to the oxygen. The optimized geometries of **9**/**13** and **9**/**14** are given in Fig. 3. Analysis of the eigenvectors corresponding to the negative eigenvalue of the force constant matrix suggests the reaction coordinate to be $0.70R_{O\cdots H}-0.66\theta_{HOC}$. Owing to the contribution of the O···H stretching mode in the reaction coordinate, the magnitude of the imaginary frequency is large (2007.3i cm^{-1}). The magnitude of the barrier for the hydrogen migration is calculated to be 80.0 kcal mol^{-1}. As is obvious from Fig. 8, **9**/**13** lies above the dissociation limits **2** and **10** and hence the probability for its formation starting from **9** is very small. The barrier for the CH_2F migration is calculated to be 112.8 kcal mol^{-1} and the TS **9**/**14** lies well above the radical dissociation limits, CH_3 + COF, CH_3CO + F, CH_2F + HCO and CH_2FCO + H. Hence, it is highly unlikely that these carbenes play any significant role in the dissociation dynamics of either CH_3COF or CH_2FCHO or in the reaction kinetics of CH_3CO + F. However, once these carbenes are formed from some other sources, they are expected to be long lived. Our study clearly reveals the stability of these carbenes due to the existence of appreciable reverse barriers for their decomposition.

4.2.3 Rearrangement to oxiranes.

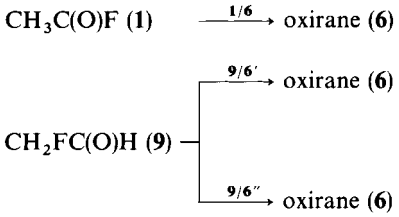

Acetyl fluoride (**1**) can isomerise to oxirane (**6**) *via* the migration of a hydrogen from the methyl carbon to the carbonyl carbon followed by a ring closure. The migration of a hydrogen creates radical centers at oxygen as well as on the migration origin. The optimized geometry of the transition structure **1**/**6** is shown in Fig. 2. The migrating hydrogen is, respectively,

Table 3 Unscaled B3LYP/6-31G(d,p) harmonic vibrational frequencies of the various saddle points on the fluoroacetaldehyde (**9**) PES; zero-point energies (ZPE) are given in kcal mol^{-1}

Species	Frequencies/cm^{-1}	ZPE
9/**12**	2066.6i, 302.3, 408.6, 657.9, 734.4, 973.8, 1093.4, 1177.1, 1179.9, 1287.7, 1421.9, 1555.7, 1912.3 3032.5, 3168.8	
9/**13**	2007.3i, 211.7, 238.8, 521.7, 747.9, 878.1, 883.0, 1101.3, 1247.2, 1370.7, 1441.9, 1465.4, 2697.8 3020.8, 3059.7	26.9
9/**14**	834.0i, 306.5, 398.7, 455.6, 705.8, 995.1, 1161.1, 1223.3, 1312.8, 1353.2, 1367.5, 1518.8, 2663.2 2910.9, 3022.7	27.7
9/**6**	724.2i, 286.4, 500.9, 594.7, 626.8, 923.3, 1081.4, 1131.5, 1233.6, 1354.0, 1465.7, 1525.3, 3045.2 3122.7, 3293.5	28.9
9/**7**	1695.6i, 51.5, 133.3, 284.8, 557.8, 747.6, 921.0, 1052.7, 1153.4, 1210.2, 1475.1, 1896.7, 3012.0 3119.3, 3277.4	27.0
9/**8**	2008.1i, 290.1, 356.6, 528.9, 568.8, 6904.4, 849.6, 858.1, 1030.9, 1079.1, 1424.5, 1638.3, 1911.6, 3155.9 3263.7	25.1
9/**15**	1672.1i, 269.0, 296.7, 535.0, 658.8, 749.6, 871.1, 976.4, 1073.7, 1219.9, 1381.0, 1512.7, 1995.9 2067.2, 2903.9	23.6
12/**15**	2036.3i, 207.5, 244.2, 423.5, 585.9, 668.6, 777.1, 997.0, 1088.2, 1236.2, 1450.7, 1778.2, 2188.2 2396.4, 3252.8	24.7
12/**16**	1602.3i, 291.7, 344.6, 480.4, 529.6, 546.4, 651.7, 924.3, 1005.2, 1108.8, 1303.4, 1745.2, 1869.0, 3394.6 3820.3	25.7
13/**4**	800.8i, 277.5, 430.1, 555.7, 642.0, 816.3, 978.3, 1020.8, 1107.3, 1275.8, 1440.7, 1526.8, 3093.0 3190.4, 3772.9	28.8
13/**12**	1225.8i, 231.5, 529.4, 652.4, 740.9, 815.1, 1023.0, 1132.9, 1277.0, 1305.1, 1377.6, 1512.2, 2095.5 3207.5, 3818.1	28.2
13/**8**	1119.1i, 359.2, 591.3, 656.6, 665.5, 772.6, 951.7, 1086.1, 1105.1, 1282.3, 1445.7, 1643.9, 1892.3 3155.2, 3248.4	26.9
13/**7**	2294.1i, 141.6, 214.2, 472.1, 492.8, 791.9, 998.3, 1109.6, 1211.5, 1261.1, 1451.4, 1502.3, 2121.6, 2854.6 3107.5	25.3
13/**15**	1616.7i, 270.5, 410.7, 616.4, 685.2, 832.3, 872.2, 1087.8, 1264.6, 1333.6, 1450.9, 1496.1, 1717.7 1807.6, 2739.6	23.7

1.164 and 1.932 Å away from the migration terminus and the origin. This migration is associated with a C—C torsional motion. The radical center CH_2 is nearly planar (HCCH = 179.4°) and the carbonyl oxygen lies in the same plane as the p-orbital of the CH_2 group. The migrating hydrogen makes a dihedral angle of 119.8° with the oxygen (HCCO = 119.8°). In other words, the carbonyl carbon has gone from sp^2 to sp^3 hybridisation, leading to a radical center at oxygen. Beyond the transition state, the reaction pathway corresponds to the formation of a bond between the two radical centers. The reaction coordinate has been identified as 0.70 ∠CCO–0.47 ∠HCC and the magnitude of the imaginary frequency equals 1353i cm^{-1} (Table 2). The barrier for this rearrangement is calculated to be 105.3 kcal mol^{-1} with a reaction endothermicity of 43.6 kcal mol^{-1}. Therefore, oxirane formation is less likely if one starts from the potential well of **1**.

Fluoroacetaldehyde (**9**) can also isomerise to oxirane either *via* the hydrogen or the fluorine migration to the carbonyl carbon. The transition structures corresponding to both the migrations have been located. However, the transition structure corresponding to fluorine migration alone is shown in Fig. 3 since the barrier height for the fluorine migration (72.2 kcal mol^{-1}) is relatively smaller than that for the hydrogen migration (79.7 kcal mol^{-1}). Isomerisation to oxirane from **9** is less endothermic (19.4 kcal mol^{-1}) and involves a lower barrier height (72.2 kcal mol^{-1}) compared with that from **1**. Oxirane formation is possible in the unimolecular dissociations of **9** and would proceed *via* the initial fluorine migration.

4.3 Molecular elimination reactions

4.3.1 Elimination of CO.

$$CH_3C(O)F\ (\mathbf{1}) \xrightarrow{1/7} CH_3F + CO\ (\mathbf{7})$$

$$CH_2FC(O)H\ (\mathbf{9}) \xrightarrow{9/7} CH_3F + CO\ (\mathbf{7})$$

Both **1** and **9** can undergo 1,1-elimination of CH_3F, yielding CO or an 1,2-elimination of HX (X = F, H) along with ketene or fluoroketene. Of all the reactions investigated here, the thermodynamically most favoured products from either of them correspond to $CH_3F + CO$. The reaction $CH_3C(O)F \rightarrow CH_3F + CO$ is the least endothermic channel from **1** and the corresponding reaction $CH_2FC(O)H \rightarrow CH_3F + CO$ is the only exothermic channel from **9**. However, the kinetic barriers involved in these channels are too high (91.7 and 80.7 kcal mol^{-1} respectively) to expect them to be significant at room temperature from the ground state. It is thus confirmed that decarboxylation is not a favourable reaction in the decomposition of acyl derivatives, CH_3COX (X = H, OH, Cl, CN, NC). The C—C distance of 2.052 Å in **1**/**7** is very long relative to the C—C distance of 1.517 Å in **1**. The C=O distance of 1.138 Å is closer to its value in the product carbon monoxide (1.138 Å) as compared with the reactant **1** (1.182 Å). The fluorine, which could be viewed as shifting from the FCO to the CH_3 fragment, is 1.864 Å from the carbonyl carbon but still 1.962 Å away from the methyl carbon. The imaginary frequency of 835i cm^{-1} (Table 2) involves, principally, the motion of fluorine with some adjustments in the positions of hydrogens in the methyl group. A qualitatively similar loose transition structure has been observed for the dissociation of formamide[34] to NH_3 and CO, for the dissociation of acetaldehyde to CH_4 and CO (ref. 4) and for the dissociation of acetyl chloride to CH_3Cl and CO.[6c] However, the transition structure **9**/**7** is different. The detaching hydrogen is still bound tightly to the carbonyl carbon and the reaction coordinate is primarily the HCC angle. It is clear from Fig. 8 that decarbonylation is also not a favourable channel from **9**.

4.3.2 Elimination of HX (X = H, F).

$$CH_3C(O)F\ (\mathbf{1}) \xrightarrow{1/8} H_2C{=}C{=}O + HF\ (\mathbf{8})$$

$$CH_2FC(O)H\ (\mathbf{9}) \xrightarrow{9/8} H_2C{=}C{=}O + HF\ (\mathbf{8})$$

$$CH_2FC(O)H\ (\mathbf{9}) \xrightarrow{9/15} HFC{=}C{=}O + H_2\ (\mathbf{15})$$

In CH_3COF, as in CH_3COCl,[5h,6c] the easiest dissociation channel is the 1,2-elimination of HF along with the formation of ketene. The associated activation barrier is 52.9 kcal mol^{-1} *via* the quite loose transition structure **1**/**8** (Fig. 2). The TS **1**/**8** is structurally comparable with that of the dehydration of acetic acid, which also gives ketene as end product ($CH_3CO_2H \rightarrow CH_2CO + H_2O$).[35] The C—F distance of 2.163 Å is long relative to the distance of 1.374 Å in **1**. The H—F distance of 1.350 Å in **1**/**8** is large compared with that in the equilibrium structure of HF (0.92 Å) and is suggestive of strong vibrational excitation in the nascent HF molecule. The C—C distance has compressed to 1.403 Å and lies between that of the ketene (1.318 Å) and **1** (1.495 Å). The detaching hydrogen from the methyl fragment is only 1.243 Å away from the methyl carbon. The C—F and H—F bonds are almost completely broken and the reaction coordinate as observed from the eigenvector of the imaginary frequency (1566i cm^{-1}) is $0.42R_{C-F} + 0.67R_{C-H}$. The C—O bond length in **1**/**8** (1.134 Å) is smaller than that in $CH_3CO^{\bullet}$ (1.180 Å) or CH_3COF (1.182 Å). Examination of the Mulliken atomic charges suggests a $CH_3CO^{\delta+}F^{\delta-}$ distribution, as found in acetyl chloride.[6d] Beyond the transition structure, the reaction will involve lengthening of the C—H bond along with a redistribution of charge in the $CH_3CO^{\delta+}$ fragment. This, therefore, indicates a vibrationally cold ketene product as observed in the case of acetyl chloride.

Both transition structures **9**/**8** and **9**/**15** shown in Fig. 3 correspond to four membered transition states. The C—O bond length in **9**/**8** (1.190 Å) is nearly the same as in **9** while the C—C distance has got compressed. The reaction involves a simultaneous cleavage of C—H and C—F bonds along with the formation of a H—F bond. Indeed, **9**/**8** can be visualised as a ketene in the biradical form with H$^{\bullet}$ and F$^{\bullet}$. The barrier for HF elimination (70.3 kcal mol^{-1}) is lower than that for H_2 elimination (93.2 kcal mol^{-1}). However, the isomerisation to 2-fluorovinyl alcohol (**12**) requires a still lower barrier (69.3 kcal mol^{-1}) and hence would compete with HF formation.

4.4 Radical dissociation pathways

$$CH_3COF\ (\mathbf{1}) \rightarrow CH_3CO^{\bullet} + F^{\bullet}\ (\mathbf{2})$$

$$CH_3COF\ (\mathbf{1}) \rightarrow CH_3^{\bullet} + FCO^{\bullet}\ (\mathbf{3})$$

$$CH_2FCHO \rightarrow CH_2FCO^{\bullet} + H^{\bullet}\ (\mathbf{10})$$

$$CH_2FCHO \rightarrow CH_2F^{\bullet} + HCO^{\bullet}\ (\mathbf{11})$$

$$CH_3CO^{\bullet} \rightarrow CH_3^{\bullet} + CO$$

$$CH_2FCO^{\bullet} \rightarrow CH_2F^{\bullet} + CO$$

Here we are concerned with the simple homolytic bond cleavages of **1** and **9**. For radical species we adopted the UB3LYP approach. The lowest bond fission reaction is the cleavage of C—C(O)X (X = F or H) single bond. More energy is required to dissociate the partially ionic C(O)—F bond. Secondary bond fission of $CH_3CO^{\bullet}$ and $CH_2FCO^{\bullet}$ is associated with barriers. For the decomposition channel of $CH_3CO^{\bullet}$ (ref. 6*c*) and $CH_2FCO^{\bullet}$ (ref. 36) a barrier of 18 kcal mol^{-1} has been estimated by us at the MP2/6-31G* level. Here we have rerun the calculations at the DFT level to obtain consistent data

and the calculated barrier heights are 16.9 and 13.6 kcal mol^{-1}, respectively.

5 PES of 1-fluoro and 2-fluorovinyl alcohols

$$H_2C{=}C(OH)F\ (4) \xrightarrow{4/8} HF + H_2C{=}C{=}O\ (8)$$
$$H_2C{=}C(OH)F\ (4) \xrightarrow{4/16} HF + HC{\equiv}COH\ (16)$$
$$HFC{=}C(OH)H\ (12) \xrightarrow{12/16} HF + HC{\equiv}COH\ (16)$$
$$HFC{=}C(OH)H\ (12) \xrightarrow{12/15} H_2 + HFC{=}C{=}O\ (15)$$

The secondary formation of ketene or its isomer HC≡COH has been studied, starting from **4** and **12**. Because the disposition of **4**/**8** is energetically below **1**/**4**, ketene formation is expected to be spontaneous from **4**. Hence the probable channels for the formation of ketene from (**1***) are

$$(1^*) \xrightarrow{1/8} (8)$$
$$(1^*) \xrightarrow{1/4} (4^*) \xrightarrow{4/8} (8^*)$$

However, the barrier for the formation of **4** is higher than that for ketene from **1**. Hence the predominant channel contributing to ketene formation will be the primary channel. It is important to discuss about the vibrational excitation of the ketene formed from **4**. In the channel

$$CH_3CO^{\cdot} + F^{\cdot} \longrightarrow CH_3COF^* \xrightarrow{1/4} H_2C{=}CF(OH^*) \xrightarrow{4/8} HF + H_2C{=}C{=}O^*$$

the C—O bond length continuously increases from **1** to **4** (1.182 Å in **1** to 1.263 Å in **1**/**4** to 1.344 Å in **4**) and later decreases from **4** to ketene (1.247 Å in **4**/**8** and 1.161 Å in ketene). Since **1**/**4** lies higher than **4**/**8**, it will roll down spontaneously to the ketene product except for the time needed for the energy redistribution. This implies that the ketene formed *via* **1**/**4** is vibrationally excited. Therefore, one would expect, in the reactions of $CH_3CO^{\cdot} + F^{\cdot}$, spontaneous ketene formation which is vibrationally cold and then a delayed ketene formation which is vibrationally hot.

The barriers for the secondary formation of fluoroketene or HC≡COH from **12** are quite high (83.4 and 99.5 kcal mol^{-1} respectively) and they lie above **9**/**12** as well as the radical dissociation limit $CH_2F + HCO$ (**10**). It is, therefore, clear that these channels do not participate significantly in the decomposition rate of **9**. The optimized structures of all these four-membered transition states are shown in Fig. 4.

6 PES of the carbenes

$$CH_3OCF\ (5) \xrightarrow{5/17} H_2C{-}O{-}CHF\ (17)$$
$$H_2FCOCH\ (14) \xrightarrow{14/17} H_2C{-}O{-}CHF\ (17)$$
$$H_2FCCOH\ (13) \xrightarrow{13/4} H_2C{=}CF(OH)\ (4)$$
$$H_2FCCOH\ (13) \xrightarrow{13/12} HFC{=}C(OH)H\ (12)$$
$$H_2FCCOH\ (13) \xrightarrow{13/7} CH_3F + CO\ (7)$$
$$H_2FCCOH\ (13) \xrightarrow{13/18} HF + H_2C{=}C{=}O\ (8)$$
$$H_2FCCOH\ (13) \xrightarrow{13/15} H_2 + HFC{=}C{=}O\ (15)$$

In spite of the low probability for carbene formation from **1** and **9**, we have investigated the possible dissociation channels from the carbenes. This will enable us to predict the possibility for their isolation and characterisation. Ylide formation from carbenes **5** and **14** involves higher barriers compared with the reverse barrier for the formation of, respectively, **1** and **9**. Thus the existence of substantial barriers establishes the fact that these carbenes are sufficiently stable. However, the transition structures for the molecular decomposition ($13 \xrightarrow{13/8} HF + H_2C{=}C{=}O$, **8**) and rearrangement ($13 \xrightarrow{13/12} HFC{=}C(OH)H$, **12**) channels lie below **9**/**13** and hence would be the favourable modes of decomposition for the carbene.

7 Dissociation kinetics of $[C_2H_3FO]$ systems

Energetically, the most favourable dissociation channel from acetyl fluoride (**1**), as in acetyl chloride, is the elimination of HF along with ketene. However, if **1** were formed in the reactions of $CH_3CO^{\cdot} + F^{\cdot}$, then the reaction rate kinetics of the energised $CH_3C(O)F^*$ will be determined by the rate of the ketene formation *via* the following pathways

$$CH_3COF\ (1) \xrightarrow{1/8} HF + H_2C{=}C{=}O\ (8)$$
$$CH_3COF\ (1) \xrightarrow{1/4} H_2C{=}CF(OH)\ (4) \xrightarrow{4/8} HF + H_2C{=}C{=}O\ (8)$$

The similarity in the geometry and charge distribution of **1**/**8** with the corresponding transition structure in acetyl chloride suggests a vibrationally excited HF and a cold ketene product. The latter channel would give rise to a delayed vibrationally hot ketene formation. Stabilisation of **4** is less effective because, at ordinary temperatures and pressures, it will immediately dissociate into ketene and HF whereas at high pressures the isomerisation **1** → **4** lies predominantly to the left. The other intermediates, *viz*., carbenes, fluorooxiranes and fluoroacetaldehyde, are not expected to contribute towards the reaction kinetics since the barriers for their formation are above the radical dissociation limit. The above result suggests $CH_3CO^{\cdot} + F^{\cdot}$ as a fast and pressure-independent association–elimination reaction.

Our *ab initio* exploration of the potential energy hypersurface for **9** shows that there is a rich variety of close lying, possibly competing, reaction channels as shown below:

$$H_2FCCHO\ (9) \xrightarrow{9/12} HFC{=}CH(OH)\ (12)$$
$$H_2FCCHO\ (9) \xrightarrow{9/8} HF + H_2C{=}C{=}O\ (8)$$
$$H_2FCCHO\ (9) \xrightarrow{9/6} \text{Fluorooxirane}\ (6)$$

In contrast to **4**, the decomposition channels arising from **12** and **6** have barriers higher than that for their formation. It is, therefore, possible to isolate these intermediates in the reactions of $CH_2FCO^{\cdot} + H^{\cdot}$ or $CH_2F^{\cdot} + HCO^{\cdot}$ at low temperatures.

Although three channels could give rise to ketene formation in the unimolecular dissociation of fluorooxirane, *viz*.,

$$\text{Fluorooxirane}\ (6) \xrightarrow{6/8} HF + HC{-}O{-}CH(\text{cyclic})$$
$$\text{Fluorooxirane}\ (6) \xrightarrow{1/6} CH_3COF\ (1) \xrightarrow{1/8} HF + H_2C{=}C{=}O\ (8)$$
$$\text{Fluorooxirane}\ (6) \xrightarrow{9/6} CH_2FCHO\ (9) \xrightarrow{9/8} HF + H_2C{=}C{=}O\ (8)$$

the channel *via* fluoroacetaldehyde is the most likely channel with a rate-limiting step of **6** → **9**. Hence, irradiation of **6** with an energy equal to the threshold for the rearrangement to **9**

should result in the ketene product. By addition, isolation of either the fluoroacetaldehyde or the acetyl fluoride intermediate is difficult as the barriers for their dissociation are lower than that for their formation from **6**. Hence, increasing the energy of fluorooxirane will result in more and more of the ketene product while increasing the pressure will reform the reactant, **6**. This, in fact, explains the non-observation of **1** and **9** in the IR multiphoton excitation studies of fluorooxirane by Quack *et al.*[10]

8 Conclusions

Electronic structure calculations have been used to characterise the [C_2, H_3, F, O] systems on their lowest singlet PES. While geometries and energies for stationary points on the PES were determined with the B3LYP (DFT) level of theory using the 6-311++G(d,p) basis set, the vibrational frequencies were obtained with a smaller basis set, 6-31G(d,p). The main features of the reaction surface are as follows.

(1) A potential energy surface consisting of ten stable intermediates has been characterised and the relative order of their thermodynamic stability is acetyl fluoride (**1**) > fluoroacetaldehyde (**9**) > 1-fluorovinyl alcohol (**4**) > 2-fluorovinyl alcohol (**12**) > fluorooxirane (**6**) > methoxyfluorocarbene (**5**) > fluoromethylhydroxycarbene (**13**) > fluoromethoxycarbene (**14**).

(2) Ketene (**8**) is expected to be the only product in the unimolecular dissociation of **1** and the accompanying hydrogen fluoride is predicted to be vibrationally hot.

(3) Combination of the reactants $CH_3CO^{\cdot} + F^{\cdot}$ to form CH_3COF occurs without a barrier and its kinetics will therefore proceed *via* an addition–elimination mechanism. Two distinct pathways involving dissociation/isomerisation have been found to be energetically open to the chemically activated initial intermediates, **1** and **4**. The above result establishes $CH_3CO^{\cdot} + F^{\cdot}$ as a fast and pressure-independent association–elimination reaction, very similar to its chlorine analog. At ambient and moderately high temperatures, the dominant reaction channels are (i) the molecular dissociation of CH_3COF (**1**) to $H_2CCO + HF$ (**8**), and (ii) the competing isomerisation of **1** to the fluorosubstituted vinyl alcohol, $CH_2{=}C(OH)F$ (**4**) and the prompt elimination of HF from **4**. It is obvious that the branching ratio depends critically on the relative energies and vibrational frequencies of the respective rate-controlling transition states **1**/**8** and **1**/**4**.

(4) Decarbonylation of **1** gives the thermodynamically most stable product but is kinetically less favourable and contributes little towards the total rate constant.

(5) Unimolecular dissociation kinetics of **9** are found to be determined by the competitive formation of **8**, **12** and **6**. Minor accessible reaction channels that result in carbene **13** and $CO + C_3DF$ have also been characterised.

(6) Carbenes do not play any significant role in the kinetics of **1** or **9**. The existence of appreciable barriers for the decomposition of carbenes suggests their kinetic stability. Owing to the weakness of the FO bond, a carbene with an OF bond is found to be unstable or non-existent.

(7) Unimolecular decomposition of **6** leads primarily to ketene product and the preferential reaction proceeds *via* the fluoroacetaldehyde intermediate with the rearrangement step (**6** → **9**) as the rate-limiting step. This explains the non-observation of **9** in the experimental decomposition studies.

(8) Many additional reaction routes and mechanisms could be interpreted on the basis of the PES, depending on the starting structures; for example, the reactivity of different carbenes.

Acknowledgements

We thank the FWO-Vlaanderen and GOA program for financial support. TLN and MTN are grateful to the Flemish Government and the KULeuven laboratory of Quantum Chemistry for supporting an "Interuniversity Program for Education in Computational Chemistry in Vietnam".

9 References

1 K. L. Kompa and R. D. Levine, *Acc. Chem. Res.*, 1994, **27**, 91.
2 (*a*) C. B. Moore and J. C. Weisshaar, *Annu. Rev. Phys. Chem.*, 1983, **34**, 525; (*b*) M. C. Chuang, M. F. Foltz and C. B. Moore, *J. Chem. Phys.*, 1987, **87**, 3855 and refs cited therein; (*c*) G. E. Scuseria and H. F. Schaefer, *J. Chem. Phys.*, 1989, **90**, 3629.
3 (*a*) A. Horowitz, C. J. Kershner and J. G. Calvert, *J. Phys. Chem.*, 1982, **86**, 3094; (*b*) A. Horowitz and J. G. Calvert, *J. Phys. Chem.*, 1982, **86**, 3105.
4 J. S. Yadav and J. D. Goddard, *J. Chem. Phys.*, 1986, **84**, 2682.
5 (*a*) M. D. Person, P. W. Kash and L. J. Butler, *J. Phys. Chem.*, 1992, **96**, 2021; (*b*) M. D. Person, P. W. Kash and L. J. Butler, *J. Chem. Phys.*, 1992, **97**, 355; (*c*) G. Olah, E. Zadok, R. Edler, D. H. Adamson, W. Kasha and G. K. Surya Prakash, *J. Am. Chem. Soc.*, 1989, **111**, 9123; (*d*) G. Natta, G. Mazzanti, G. Pregoglia, M. Binaghi and M. Peraldo, *J. Am. Chem. Soc.*, 1960, **82**, 4742; (*e*) N. Kogure, T. Ono and F. Watari, *J. Mol. Struct.*, 1993, **296**, 1; (*f*) S. Deshmukh and W. P. Hess, *J. Chem. Phys.*, 1994, **100**, 6429; (*g*) S. Deshmukh and W. P. Hess, *J. Phys. Chem.*, 1994, **98**, 12535; (*h*) P. R. Winter, B. Rowland, W. P. Hess, J. G. Radziszewski, M. R. Nimlosand and G. B. Ellison, *J. Phys. Chem. A*, 1998, **102**, 3238.
6 (*a*) R. Sumathi and A. K. Chandra, *J. Chem. Phys.*, 1993, **99**, 6531; (*b*) B. Rowland and W. P. Hess, *J. Phys. Chem. A*, 1997, **101**, 8049; (*c*) R. Sumathi and A. K. Chandra, *Chem. Phys.*, 1994, **181**, 73; (*d*) R. Sumathi and M. T. Nguyen, *J. Phys. Chem. A*, 1998, **102**, 8150.
7 (*a*) B. R. Weiner and R. N. Rosenfeld, *J. Phys. Chem.*, 1988, **92**, 4640; (*b*) D. E. Klimek and M. J. Berry, *Chem. Phys. Lett.*, 1973, **20**, 141; (*c*) K. Morokuma, S. Kato and K. Hirao, *J. Chem. Phys.*, 1980, **72**, 1800.
8 (*a*) Y. S. Choi, P. Teal and C. B. Moore, *J. Opt. Soc. Am. B*, 1990, **7**, 1829; (*b*) Y. S. Choi and C. B. Moore, *J. Chem. Phys.*, 1991, **94**, 5414; (*c*) Y. S. Choi and C. B. Moore, *J. Chem. Phys.*, 1992, **97**, 1010; (*d*) Y. S. Choi and C. B. Moore, *J. Chem. Phys.*, 1995, **103**, 9981.
9 (*a*) J. D. Goddard and H. F. Schaefer, *J. Chem. Phys.*, 1990, **93**, 4907; (*b*) K. Kamiya and K. Morokuma, *J. Chem. Phys.*, 1991, **94**, 7287.
10 H. Hollenstein, D. Luckhaus, J. Pochert, M. Quack and G. Seyfang, *Angew. Chem., Int. Ed. Engl.*, 1997, **36**, 140.
11 T. K. Ha, J. Pochert and M. Quack, *J. Phys. Chem. A*, 1998, **102**, 5241.
12 T. Schaefer, T. A. Wildman and R. Sebastian, *J. Mol. Struct. (Theochem)*, 1982, **6**, 93.
13 V. J. Klimkowski, P. Pulay, J. D. Ewbank, D. C. Mckean and L. Schafer, *J. Comput. Chem.*, 1984, **5**, 517.
14 J. De Smedt, F. Vanhuoteghen,, C. Van Alsenoy, H. J. Geise and L. Schafer, *J. Mol. Struct. (Theochem)*, 1992, **91**, 289.
15 K. B. Wiberg, C. M. Hadad, P. R. Rablen and J. Cioslowski, *J. Am. Chem. Soc.*, 1992, **114**, 8644.
16 J. W. Ochterski, G. A. Petersson and K. B. Wiberg, *J. Am. Chem. Soc.*, 1995, **117**, 11299.
17 M. R. Zachariah, P. R. Westmoreland, D. R. Burgress, W. Tsang and C. F. Melius, *J. Phys. Chem.*, 1996, **100**, 8737.
18 M. W. Wong, *Chem. Phys. Lett.*, 1996, **256**, 391.
19 R. Sumathi and A. K. Chandra, *Chem. Phys.*, 1992, **165**, 257.
20 R. Sumathi and M. T. Nguyen, *J. Phys. Chem. A*, 1998, **102**, 412.
21 M. M. Maricq, J. C. Ball, A. M. Straccia and J. J. Szente, *Int. J. Chem. Kinet.*, 1997, **29**, 421.
22 (*a*) M. J. Frisch, G. W. Trucks, M. Head-Gordon, P. M. W. Gill, M. W. Wong, J. B. Foresman, B. G. Johnson, H. B. Schlegel, M. A. Robb, E. S. Replogle, R. Gompertz, J. L. Andres, K. Raghavachari, J. S. Binkley, C. Gonzalez, R. J. Martin, D. J. Fox, D. J. Defrees, J. Baker, J. J. P. Stewart and J. A. Pople, Gaussian 94, Gaussian Inc., Pittsburgh PA, 1994; (*b*) A. D. Becke, *J. Chem. Phys.*, 1993, **98**, 5648; (*c*) C. Lee. W. Yang and R. G. Parr, *Phys. Rev. B*, 1988, **37**, 785.
23 (*a*) L. Pierce, *Bull. Am. Phys. Soc. Ser. II*, 1956, **1**, 198; (*b*) L. Pierce and L. C. Krisher, *J. Chem. Phys.*, 1959, **31**, 875.
24 (*a*) R. W. Kilb, C. C. Lin and E. B. Wilson, *J. Chem. Phys.*, 1957, **26**, 1695; (*b*) J. D. Swalen and C. C. Costain, *J. Chem. Phys.*, 1959, **31**, 1562; (*c*) R. Nelson and L. Pierce, *J. Mol. Spectrosc.*, 1965, **18**, 344; (*d*) M. D. Harmony, V. W. Laurie, R. L. Kuczkowski, R. H. Schwendeman, D. A. Ramsay, F. J. Lovas, W. J. Lafferty and A. G. Maki, *J. Phys. Chem. Ref. Data*, 1979, **8**, 619.
25 (*a*) T. Iijima and M. Kimura, *Bull. Chem. Soc. Jpn.*, 1969, **42**, 2159; (*b*) T. Iijima, *Bull. Chem. Soc. Jpn.*, 1972, **45**, 3526; (*c*) C.

Kato, S. Konaka, T. Iijima and M. Kimura, *Bull. Chem. Soc. Jpn.*, 1969, **42**, 2148.
26 (*a*) D. C. McKean, J. L. Duncan and L. Batt, *Spectrochim. Acta A*, 1973, **29**, 1037; (*b*) D. C. McKean, *Spectrochim. Acta A*, 1975, **31**, 861; (*c*) R. Nakagaki and I. Hanazaki, *J. Phys. Chem.*, 1982, **86**, 1501.
27 H. V. Phan and J. R. Durig, *J. Mol. Struct.* (*Theochem*), 1990, **209**, 333.
28 D. A. Dixon and B. E. Smart, *J. Phys. Chem.*, 1991, **95**, 1609.
29 (*a*) J. R. Sodeau and E. K. C. Lee, *Chem. Phys. Lett.*, 1978, **57**, 71; (*b*) S. N. Ahmed, M. L. McKee and P. B. Shevlin, *J. Am. Chem. Soc.*, 1985, **107**, 1320.
30 D. Sulzle, T. Drewello, B. L. M. van Baar and H. Schwarz, *J. Am. Chem. Soc.*, 1988, **110**, 8330.
31 (*a*) R. S. Sheridan and M. A. Kasselmayer, *J. Am. Chem. Soc.*, 1984, **106**, 436; (*b*) M. A. Kasselmayer and R. S. Sheridan, *J. Am. Chem. Soc.*, 1986, **108**, 99.
32 J. S. Yadav and J. D. Goddard, *J. Chem. Phys.*, 1986, **85**, 3975.
33 A. Tachibana, M. Koizumi, I. Okazaki, H. Teramae and T. Yamabe, *Theor. Chim. Acta*, 1987, **71**, 7.
34 T. Takumoto, K. Saito and A. Imamura, *J. Phys. Chem.*, 1985, **89**, 2286.
35 M. T. Nguyen, D. Sengupta, G. Raspoet and L. G. Vanquickenborne, *J. Phys. Chem.*, 1995, **99**, 11883.
36 A. Srivatsava, E. Arunan, G. Manke II, D. W. Setser and R. Sumathi, *J. Phys. Chem. A*, 1998, **102**, 6406.

Paper 8/07117I